Electronic Supplementary Material (ESI) for New Journal of Chemistry.

NiCrO/MCu111 interface sites for synergistic catalysis to water splitting

Tonghui Mu, Dongxu Tian*

School of Chemistry, Dalian University of Technology, No.2 Linggong Road, Dalian City, Liaoning Province, P. R. China, 116024

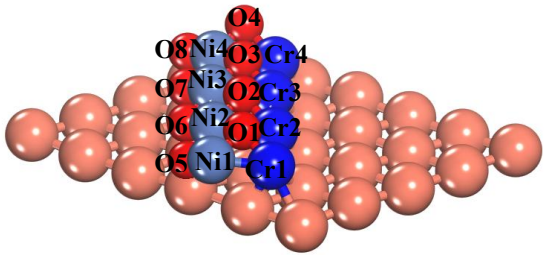

Figure S1 the labellized structure of NiCrO/Cu111.

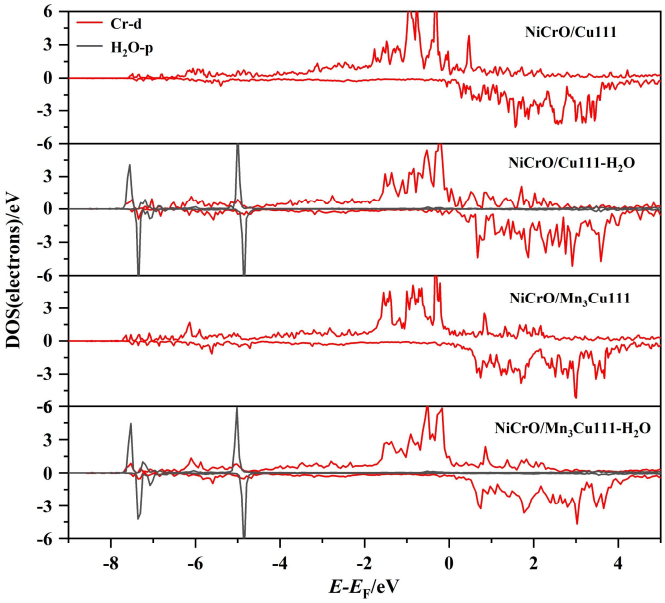

Figure S2-1 PDOS plot of the p orbital of H_2O and the 3d orbital of Cr atoms before and after H_2O adsorption.

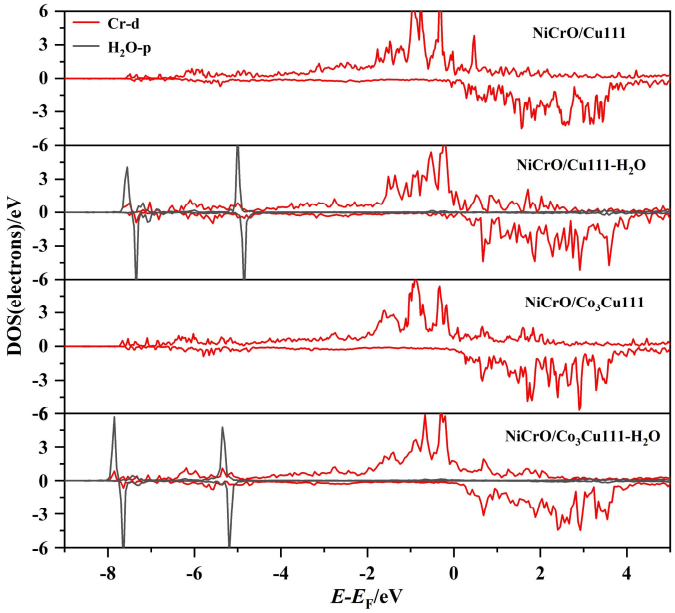

Figure S2-2 PDOS plot of the p orbital of H_2O and the 3d orbital of Cr atoms before and after H_2O adsorption.

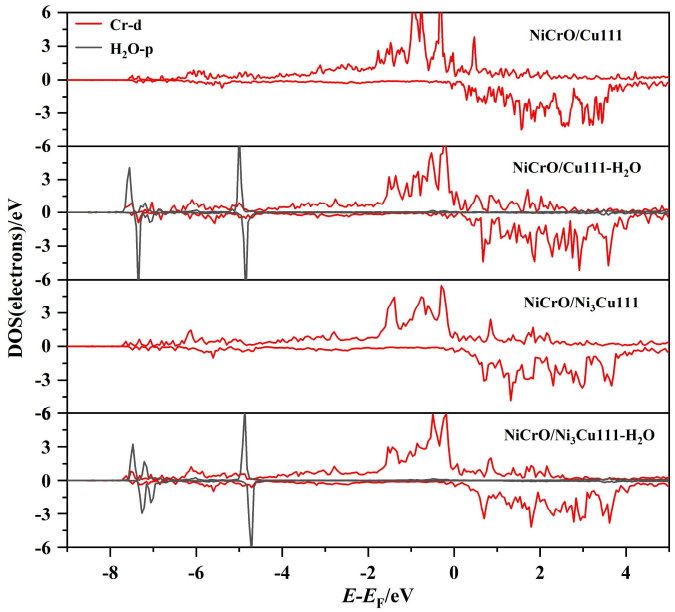

Figure S2-3 PDOS plot of the p orbital of H_2O and the 3d orbital of Cr atoms before and after H_2O adsorption.

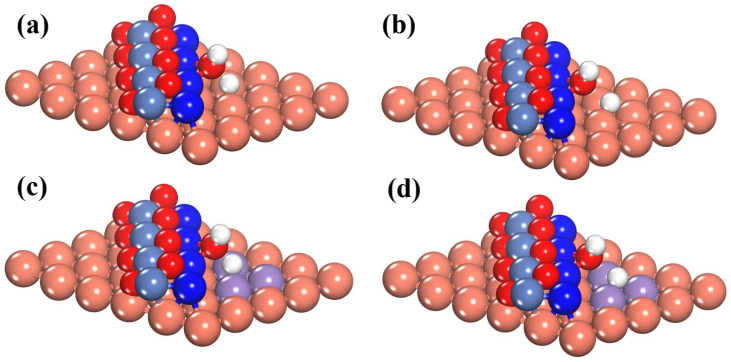

Figure S3. The H_2O dissociation transition state structures (a) and (c); The H_2O dissociation product structures (b) and (d). Red: O; White: H; Blue: Cr; Light blue: Ni and purple: transition metal atom

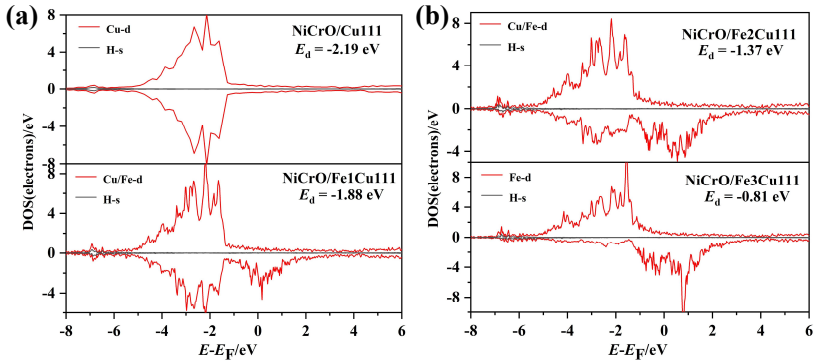

Figure S4-1 PDOS plot of the s orbital of H and the 3d orbital of Cr atoms. (a) NiCrO/Cu111 and NiCrO/Fe1Cu111; (b)NiCrO/Fe2Cu111 and NiCrO/Fe3Cu111

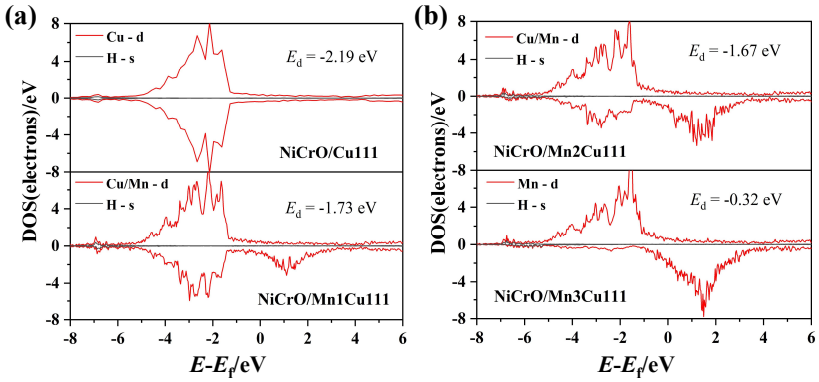

Figure S4-2 PDOS plot of the s orbital of H and the 3d orbital of Cr atoms. (a) NiCrO/Cu111 and NiCrO/Mn1Cu111; (b)NiCrO/Mn2Cu111 and NiCrO/Mn3Cu111

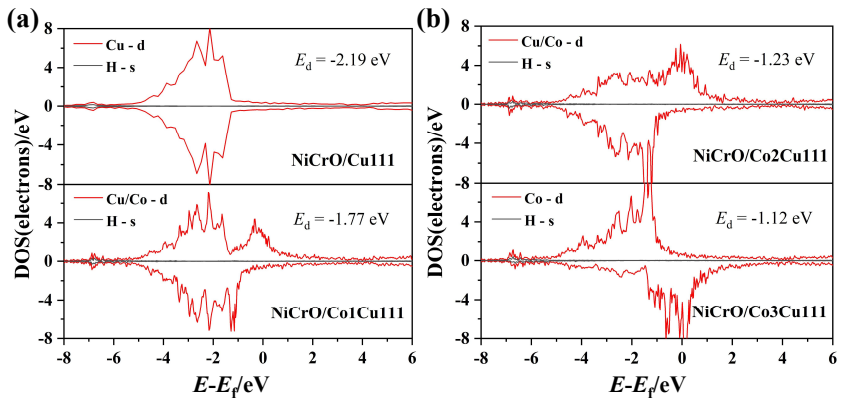

Figure S4-3 PDOS plot of the s orbital of H and the 3d orbital of Cr atoms. (a) NiCrO/Cu111 and NiCrO/Co1Cu111; (b)NiCrO/Co2Cu111 and NiCrO/Co3Cu111

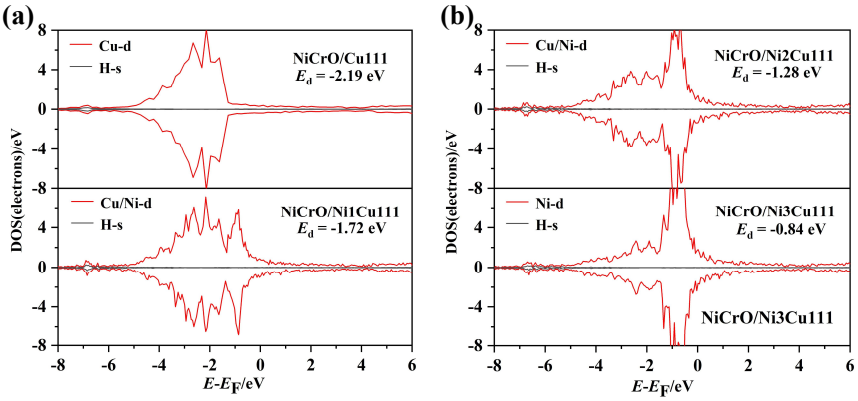

Figure S4-4 PDOS plot of the s orbital of H and the 3d orbital of Cr atoms. (a) NiCrO/Cu111 and NiCrO/Ni1Cu111; (b)NiCrO/Ni2Cu111 and NiCrO/Ni3Cu111

Table S1 The net charge results of NiCrO/Cu111.

Atoms	Bader charge/|e|
O1	-1.034
O2	-1.032
O3	-1.029
O4	-1.043
O5	-0.815
O6	-0.815
O7	-0.814
O8	-0.814
Cr1	0.942
Cr2	0.936
Cr3	0.931
Cr4	0.931
Ni1	0.841
Ni2	0.842
Ni3	0.840
Ni4	0.840

Table S2-1 Bader charge and d-band center of NiCrO/MCu111 (M=Mn, Fe, Co and Ni)

Systems	Site	Bader charge/|e|	*d*-band center/eV
NiCrO/Cu	Cu	0.006	-2.191
	Cu	0.053	
	Cu	0.027	
NiCrO/Fe1Cu	Cu	-0.024	-1.885
	Fe	0.381	
	Cu	-0.061	
NiCrO/Fe2Cu	Fe	0.218	-1.368
	Fe	0.305	
	Cu	-0.090	
NiCrO/Fe3Cu	Fe	0.179	-0.811
	Fe	0.209	
	Fe	0.264	
NiCrO/Cu	Cu	0.006	-2.191
	Cu	0.053	
	Cu	0.027	
NiCrO/Mn1Cu	Cu	-0.087	-1.732
	Mn	0.598	
	Cu	-0.133	
NiCrO/Mn2Cu	Mn	0.533	-1.166
	Mn	0.503	
	Cu	-0.211	
NiCrO/Mn3Cu	Mn	0.451	-0.319
	Mn	0.404	
	Mn	0.410	

Table S2-2 Bader charge and d-band center of NiCrO/MCu111 (M=Mn, Fe, Co and Ni)

Systems	Site	Bader charge/|e|	*d*-band center/eV
NiCrO/Cu	Cu	0.006	-2.191
	Cu	0.053	
	Cu	0.027	
NiCrO/Co1Cu	Cu	0.031	-1.771
	Co	0.083	
	Cu	0.011	
NiCrO/Co2Cu	Co	-0.066	-1.235
	Co	-0.044	
	Cu	0.006	
NiCrO/Co3Cu	Co	0.027	-1.117
	Co	0.062	
	Co	0.108	
NiCrO/Cu	Cu	0.006	-2.191
	Cu	0.053	
	Cu	0.027	
NiCrO/Ni1Cu	Cu	-0.002	-1.721
	Ni	0.026	
	Cu	-0.024	
NiCrO/Ni2Cu	Ni	0.015	-1.283
	Ni	0.045	
	Cu	-0.058	
NiCrO/Ni3Cu	Ni	0.045	-0.842
	Ni	0.011	
	Ni	0.005	

Table S3 The net charge data of H_2O adsorbed on bridge of NiCrO/Cu111.

Atoms	Bader charge/|e|
O1	-1.040
O2	-1.049
O3	-1.041
O4	-1.061
O5	-0.816
O6	-0.810
O7	-0.814
O8	-0.814
O9	-1.332
Cr1	0.889
Cr2	1.035
Cr3	1.041
Cr4	0.880
Ni1	0.840
Ni2	0.844
Ni3	0.846
Ni4	0.839
H1	0.696
H2	0.630

Table S4. The structure parameters of adsorbed *OH, *H in product states and the dissociation reaction energies (ΔE).

Systems	dO-Cr1/Å	dO-Cr2/Å	dH-O1/Å	dH-O2/Å	ΔEreac/eV
NiCrO/Mn1Cu	1.938	1.976	0.979	2.814	-0.79
NiCrO/Fe1Cu	1.939	1.972	0.979	2.851	-0.84
NiCrO/Co1Cu	1.948	1.938	0.979	2.774	-0.97
NiCrO/Ni1Cu	1.963	1.963	0.979	2.712	-0.83
NiCrO/Mn2Cu	1.960	1.956	0.979	2.789	-1.02
NiCrO/Fe2Cu	1.982	1.978	0.980	2.792	-0.96
NiCrO/Co2Cu	1.947	1.952	0.981	2.454	-1.10
NiCrO/Ni2Cu	1.948	1.955	0.978	2.670	-0.93
NiCrO/Mn3Cu	1.984	1.983	0.978	2.657	-1.21
NiCrO/Fe3Cu	1.982	1.981	0.979	2.634	-1.07
NiCrO/Co3Cu	1.959	1.940	0.978	2.731	-1.25
NiCrO/Ni3Cu	1.944	1.948	0.980	2.870	-1.05
NiCrO/Cu	1.967	1.965	0.979	2.749	-0.68

Table S5 Adsorption energies of H*(ΔE_{H*}) and d-band centers of active sites at different NiCrO/MCu111 interfaces

Systems	H* adsorbed site	ΔE_{H*}/eV	*d*-band center/eV
NiCrO/Mn1Cu	fcc	-0.42	-1.733
NiCrO/Fe1Cu	fcc	-0.57	-1.166
NiCrO/Co1Cu	fcc	-0.62	-0.319
NiCrO/Ni1Cu	fcc	-0.56	-1.885
NiCrO/Mn2Cu	fcc	-0.63	-1.368
NiCrO/Fe2Cu	fcc	-0.68	-0.811
NiCrO/Ni2Cu	fcc	-0.73	-1.235
NiCrO/Mn3Cu	fcc	-0.73	-1.117
NiCrO/Fe3Cu	fcc	-0.81	-1.721
NiCrO/Co3Cu	fcc	-0.72	-1.283
NiCrO/Ni3Cu	fcc	-0.84	-0.842
NiCrO/Cu	fcc	-0.36	-2.191

Table S6 Adsorption energies ΔE_{ads} (eV), H-O-H bond angles θ (°), O-Cr bond lengths and H-OH bond lengths (Å) for H_2O adsorption states on NiMnO/Cu111, NiFeO/Cu111 and NiCoO/Cu111

Slab	$d_{O\text{-}Cr1}$/Å	$d_{O\text{-}Cr2}$/Å	$d_{H\text{-}O1}$/Å	$d_{H\text{-}O2}$/Å	$\theta_{(H\text{-}O\text{-}H)}$/°	ΔE_{H2O*}/eV	ε_d
NiMnO/Cu	2.44	2.38	0.98	0.99	108.89	-0.93	-0.62
NiFeO/Cu	2.31	2.29	0.98	0.99	110.18	-0.79	-1.13
NiCoO/Cu	2.28	2.29	0.98	0.99	109.54	-0.64	-1.17

Table S7 Geometric parameters and the imaginary frequency (cm^{-1}) of the H_2O dissociation transition states on NiMnO/Cu111, NiFeO/Cu111 and NiCoO/Cu111.

Slab	$d_{O\text{-}Cr1}$/Å	$d_{O\text{-}Cr2}$/Å	$d_{H\text{-}O1}$/Å	$d_{H\text{-}O2}$/Å	$\theta_{(H\text{-}O\text{-}H)}$/°	f/i/cm^{-1}	ΔE_{HO*}/eV
NiMnO/Cu	2.15	2.16	0.98	1.40	113.50	1106.46	-0.88
NiFeO/Cu	2.11	2.11	0.98	1.38	116.16	1169.87	-0.78
NiCoO/Cu	2.08	2.07	0.98	1.40	115.34	1122.82	-0.47